Kafkas Univ Vet Fak Derg
24 (3): 393-400, 2018
DOI: 10.9775/kvfd.2017.19052

Kafkas Universitesi Veteriner Fakultesi Dergisi
Journal Home-Page: http://vetdergikafkas.org
Online Submission: http://submit.vetdergikafkas.org

Research Article

Radiosynthesis and Biodistribution of ^{99m}Tc-Trimethoprim: A Novel Radiolabeled Antibiotic for Bacterial Infection Imaging Using Experimental Animals

Hasan DEMİROĞLU [1] Gökçen TOPAL [2] Yasemin PARLAK [2] Fikriye Gül GÜMÜŞER [2]
Elgin Uluer TÜRKÖZ [3] Volkan TEKİN [4] Buket ATEŞ [1] Perihan ÜNAK [4] Uğur AVCIBAŞI [1]

[1] Department of Chemistry, Faculty of Art and Science, Manisa Celal Bayar University, TR-45140 Manisa - TURKEY
[2] Department of Nuclear Medicine, Manisa Celal Bayar University, Faculty of Medicine, TR-45140 Manisa - TURKEY
[3] Department of Histology and Embryology, Manisa Celal Bayar University, Faculty of Medicine, TR-45140 Manisa - TURKEY
[4] Institute of Nuclear Sciences, Ege University, Department of Nuclear Applications, TR-35100 Bornova, İzmir - TURKEY

Article Code: KVFD-2017-19052 Received: 24.11.2017 Accepted: 28.01.2018 Published Online: 28.01.2018

How to Cite This Article

Demiroğlu H, Topal G, Parlak Y, Gümüşer FG, Türköz EU, Tekin V, Ateş B, Ünak P, Avcıbaşı U: Radiosynthesis and biodistribution of ^{99m}Tc-trimethoprim: A novel radiolabeled antibiotic for bacterial infection imaging using experimental animals. *Kafkas Univ Vet Fak Derg,* 24 (3): 393-400, 2018 *(Article in Press).* DOI: 10.9775/kvfd.2017.19052

Abstract

In the present article, we focused on the radiolabeling and evaluation of ^{99m}Tc–TMH complex as a potential candidate for infection imaging *in vivo*. For this; Trimethoprim (TMH) used to treat bacterial infections was investigated to label with ^{99m}Tc. Labeling was performed using thin (II) chloride as a reducing agent at room temperature for 1 h and radiochemical analysis involved thin layer radiochromatography (TLRC) and high pressure liquid radiochromatograpy (HPLRC) methods. The stability of labeled antibiotic was checked in the presence of rat blood serum at 37°C up to 180 min. The maximum radiolabeling yield was found to be 96±2% and remained constant at more than 85±1% even in rat serum for 180 min after radiolabeling. Static image of ^{99m}Tc-TMH in male rats demonstrated that important radiation signals are present in the infected site at first glance in 30 min. After 30 min the uptake of the ^{99m}Tc-TMH as ID/g% in the infected muscle (INM) and normal muscle (NM) of the rats were 7.5±1.5% and 5.00±1.2%, respectively. In the INM/NM ratio a desirable behavior was observed as the values for the INM/NM increased up to 10.6. ^{99m}Tc-TMH prepared with high yield is able to localize well in the bacterially infected muscle of the rats. As a result, ^{99m}Tc-TMH may be developed as a radiopharmaceutical agent to distinguish infection from inflammation by nuclear imaging.

Keywords: *Trimethoprim, ^{99m}Tc, Infection imaging agent, S. aureus*

^{99m}Tc-Trimethoprim'in Radyosentezi ve Biyodağılımı: Deney Hayvanları Kullanılarak Bakteriyel Enfeksiyon Görüntüleme İçin Yeni Bir Radyoişaretli Antibiyotik

Öz

Bu çalışmada *in vivo* enfeksiyon görüntüleme için potansiyel bir aday olarak ^{99m}Tc-TMH'ı değerlendirdik ve radyosentezi üzerine odaklandık. Bunun için bakterilerden kaynaklı enfeksiyonların tedavisinde kullanılan Trimethoprim (TMH) ^{99m}Tc ile işaretlenmiştir. İşaretlenme oda sıcaklığında 1 saat süreyle bir indirgenme ajanı olan Sn(II)Cl2 kullanılarak gerçekleştirilmiş ve ince tabaka radyokromatografi (TLRC) ve yüksek basınçlı sıvı radyokromatografisi (HPLRC) metodlarını içeren radyokimyasal analizler yapılmıştır. İşaretli antibiyotiğin sıçan kan serumundaki kararlılığı 37°C'de 180. dk.'ya kadar kontrol edilmiştir. Maksimum bağlanma verimi %96±2 olarak bulunmuş ve işaretli antibiyotiğin işaretlenmeden sonra 180 dk süresi içinde sıçan serumunda %85±1'in üzerindeki bir oranda sabit kaldığı görülmüştür. Dişi sıçanlardaki ^{99m}Tc-TMH'ın statik görüntüsü ilk 30 dk içinde enfeksiyon bölgesinde işaretli antibiyotiğin önemli bir radyasyon sinyali verdiğini göstermiştir. 30 dk sonra ^{99m}Tc-TMH'ın enfekte kas (INM) ve normal kas (NM) daki tutulum değerleri sırasıyla %7.5±1.5 ve %5.00±1.2 dir. INM/NM oranı 10.6 değerine kadar attığı için INM/NM oranında makul bir artış gözlenmiştir. Yüksek verimle hazırlanmış ^{99m}Tc-TMH bakteriler tarfından enfekte edilmiş sıçan kaslarında lokalize olabilmektedir. Sonuç olarak ^{99m}Tc-TMH nükleer görüntülemede kullanılabilecek bir radyofarmasötik olarak geliştirilebilir.

Anahtar sözcükler: *Trimethoprim, ^{99m}Tc, Enfeksiyon Görüntüleme Ajanı, S. aureus*

İletişim (Correspondence)
+90 236 2013157 Fax: +90 236 2412158
ugur.avcibasi@gmail.com; ugur.avcibasi@cbu.edu.tr

INTRODUCTION

Trimethoprim (TMP) given in *Fig. 1* is frequently used as human medicines to treat bronchitis and urinary tract infections. In most circumstance, they are used in combination as chemical therapy agents and growth promoters in veterinary [1-15].

In the early stages of infectious diseases, the diagnostic roles of the currently used techniques, such as ultrasound technology (UST), computerized tomography (CT) and magnetic resonance imaging (MRI), have proven unsatisfactory. However, nuclear medicine scintigraphy (NMS) has shown promise in the precise and early diagnosis of infection and its discrimination from inflammation. NMS has considerably improved the rate of accurate diagnosis and to a large extent decreased the chances of incorrect identification [16,17]. Trimethoprim is rapidly absorbed following oral administration. Trimethoprim exists in the blood as unbound, protein-bound and metabolized forms. Trimethoprim is metabolized in vitro to 11 different metabolites, of which, five are glutathione adducts and six are oxidative metabolites, including the major metabolites, 1- and 3-oxides and the 3- and 4-hydroxy derivatives [18].

Technetium-99m (^{99m}Tc)-labeled radiopharmaceuticals have further potentiated the diagnostic capabilities of NMS in the topical decade specifically for the diagnosis of deep tissue infection and its discrimination from inflammation. Recently, some novel specific infection radiotracers have been developed, including ours, for localization and discrimination of infection from inflammation. The effectiveness of these radiopharmaceuticals has encouraged the development of novel and more specific agents [19-26].

A novel approach using bacterially binding radiolabeled antibiotics was evaluated with different researchers. ^{99m}Tc-labeled ciprofloxacin, alafosfalin, enrofloxacin, gatifloxacin, cefepime, ceftriaxone, levofloxacin, and cefotaxime were evaluated as an infection imaging agent [27].

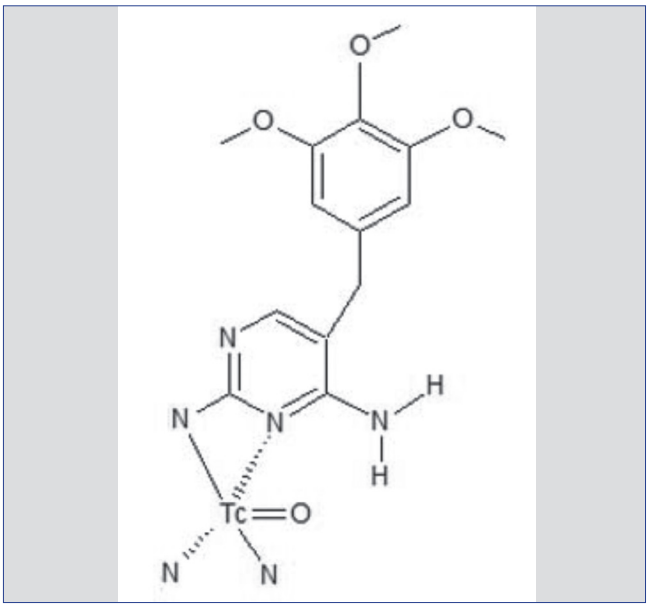

Fig 1. Chemical structure of ^{99m}Tc-TMH

Uyaroğlu et al.[28] have reported that the ^{99m}Tc-SMX would be developed as a radiopharmaceutical agent to distinguish infection from inflammation by nuclear imaging.

In this study, TMH was labeled with technetium-99m pertechnetate using $SnCl_2{\cdot}2H_2O$ as reducing agent. The labeling efficiency depends on ligand/reductant ratio, pH, and volume of reaction mixture. Radiochemical purity and stability of ^{99m}Tc-TMH was determined by thin layer radiochromatography (TLRC) and HPLRC. Biodistribution and scintigraphy studies of ^{99m}Tc-TMP were performed in a model of bacterial infection in Albino Wistar rats. A significantly higher accumulation of ^{99m}Tc-TMH was seen at sites of *S. aureus* infected animals.

MATERIAL and METHODS

All chemicals and solvents were used without further purification. TMH, stannous tartrate and other chemicals were purchased from Sigma-Aldrich (USA). ^{99m}Tc was eluted from the molybdenum-99 (^{99}Mo)/^{99m}Tc generator from Eczacıbaşı Monrol (Turkey) in the Nuclear Medicine Department of Manisa Celal Bayar University. Dose Calibrator (Atomlab 100, Biodex Medical Systems) was used for counting radioactive samples. *Staphylococcus aureus* (SA) bacteria were obtained from Pharmaceutical Microbiology Department of Manisa Celal Bayar University. The Animal Ethics Committee of the Manisa Celal Bayar University gave approval for the animal experiments (Number: 28, 26/04/2016 dated).

Radiolabeling of TMH with ^{99m}Tc

In the labeling of TMH with ^{99m}Tc, 100 µg (100 µL) of TMP was added to a vial. About 5 µg (50 µL) of $SnCl_2.2H_2O$ was added into the vial as a reducing agent and pH of this mixture was adjusted to 10 by using 1.0 M of NaOH solution. Then, 37MBq (1 mCi) of $Na^{99m}TcO_4$ was added into the vial and incubated at room temperature for 1 h.

Quality Control Studies

Thin-layer Radiochromatography: For the thin-layer radiochromatography studies (TLRC), TLC aluminum sheets (Merck, 20 × 20 cm code: 5552) were used and acetone-water (9:1) was used as the mobile phase. The TLRC technique was performed to determine the retention values of the radiolabeled product. Each TLRC sheets was evaluated by the Cyclone Plus Storage Phosphor System. Radiochromatograms of radioactive components were given in *Fig. 2*.

High Pressure Liquid Radio Chromatography (HPLRC): A high pressure gradient HPLRC system (LC-20AD quaternary

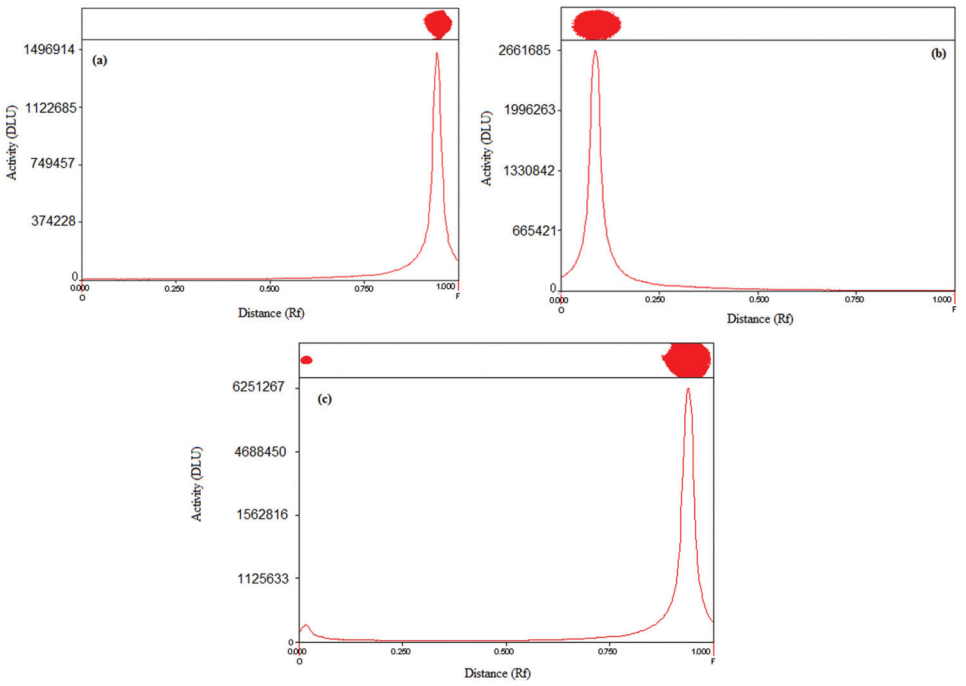

Fig 2. The radiochromatograms of $^{99m}Tc^{+7}$ (a) ^{99m}Tc-TMH (b) and $^{99m}Tc^{+4}$ (c) developed with acetone/water (9:1)

Table 1. *Biodistribution of ^{99m}Tc-TMH in infected rats 30, 120 and 240 min post-injection (%ID/g)*

Organs	%ID/g		
	30 min.	**120 min.**	**240 min.**
Heart	25.33±2.28	4.07±0.55	2.87±0.45
Lungs	136.67±7.36	11.91±2.14	10.52±1.85
Liver	165.67±27.45	7.55±4.20	6.45±1.23
Kidneys	66.66±9.83	57.67±21.36	51.69±4.51
Small intesitine	12.34±7.11	8.59±4.33	5.35±2.26
Large intestine	38.43±22.02	4.54±0.29	8.44±3.83
Stomach	17.98±3.01	208.33±11.77	61.70±1.83
Blood	26.19±12.56	7.89±1.45	3.39±0.15
Normal muscle	5.00±1.20	1.57±0.39	1.88±0.99
Infected muscle	7.46±1.50	5.30±0.45	3.39±1.89

Values expressed as the mean ± standard deviation, n=3

pump, SPD-10A UV detector, SIL, 20A-HT auto sampler) was used. HPLRC analysis conditions; C18-ODS column (250 9 4.6 mm I.D. Gl sciences Inc.) mobile phase; MeOH (0.1% TFA)/THF (80:20), flow rate: 1 mL/min., wavelenght: 254 nm. HPLRC chromatograms of ^{99m}Tc-TMH were given in *Fig. 3*. In addition, retention times (R_t) of $^{99m}TcO_4^-$ and ^{99m}Tc-TMH were given in *Table 1*.

Effect of pH: The effect of pH on the labelling efficiency was shown in *Fig. 4*. TMH (100 µg) was labelled at different pH (1, 3, 7, 10 and 13) using 5 µg of $SnCl_2.H_2O$ as reducing agent. At pH 3 the compound was poorly labelled and with increase in pH the labelling efficiency increased. At pH 10 maximum labelling >90% was noted, hence further experiments were performed at this pH.

Stability of ^{99m}Tc-TMH in the Rat Blood Serum: The stability of radiolabeled compound in rat serum was determined by incubating 100 µg/100 µL of the labeled compound with 300 µL of rat blood serum at 37°C. The aliquots were analyzed in time intervals of 0, 30, 60, 120, and 180 min by TLRC technique after labeling. Results of stability study were given in *Fig. 5*.

Animal Studies

Two groups of 3 female Albino Wistar rats infected with SA (200-250 g) were used for animal studies. Induction of infection model *Staphylococus aureus* was used to create infection model. Intramuscularly injected with 200 µL (1×10^8 CFU/mL) *S. aureus* suspension into the right thigh

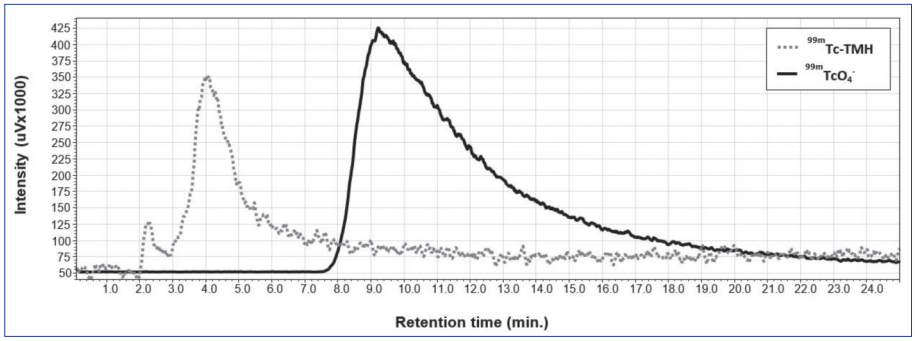

Fig 3. HPLC chromatograms of ^{99m}Tc-TMH

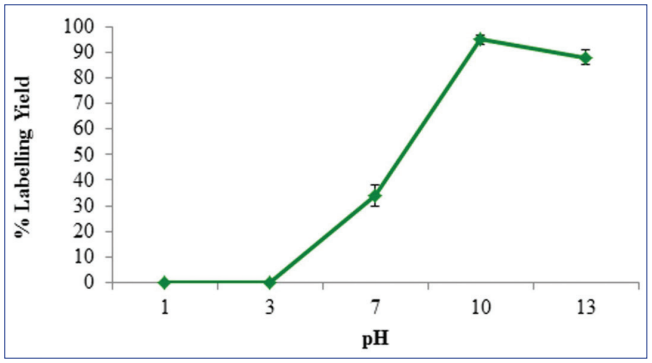

Fig 4. Labelling yields at different pH. Reaction condition: 100 µg TMH, 5 µg $SnCl_2$ and ^{99m}Tc (1 mCi) at room temperature for 60 min

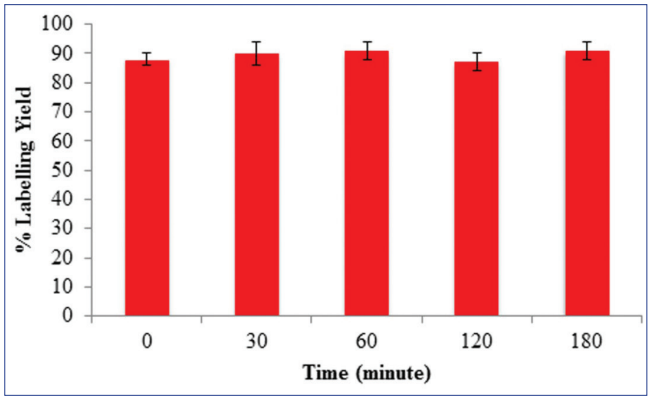

Fig 5. Stability of ^{99m}Tc-TMH in rat serum

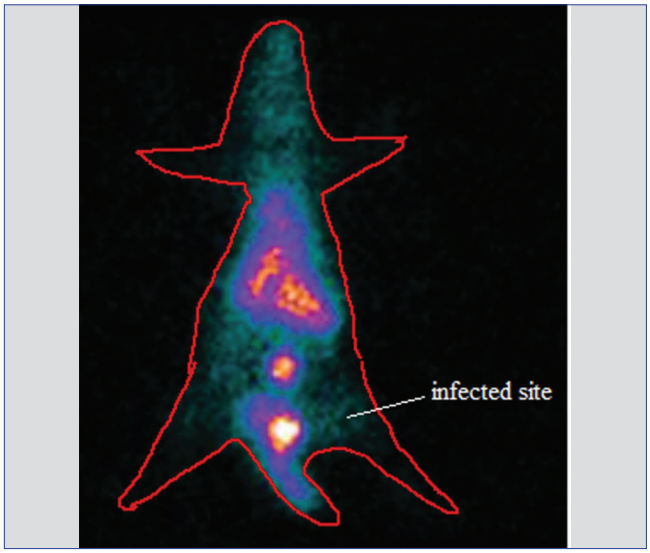

Fig 6. Static scintigram of ^{99m}Tc-TMH, which was administered to a rat via the tail vein in 30 min (The mixture of xylazine and ketamine anesthesia was used in the scintigraphy studies. Static image was obtained from posterior projection following the administration of the ^{99m}Tc-TMH)

muscle. Then the infection was allowed to develop for 48 h.

Scintigraphic Imaging Studies

After the infection focus was allowed to develop for 48 h, swelling appeared, and gamma scintigraphy studies were performed. Rat infected with SA was intravenously injected with 37 MBq of ^{99m}Tc-TMH via tail vein, and during the scintigraphy studies animal was under anesthetize with Ketamine/Xylazin cocktail. The scintigraphic images were obtained with a dual head gamma camera (Infinia General Electric) equipped with a low energy, high-resolution collimator viewing the whole body of rats and handheld USB-Gamma Camera (Crystal Cam). After administration of radiopharmaceuticals, serial static images were acquired in a 256 × 256 matrix for 60 s each, at different time intervals (5, 15, 30, 120 and 240 min post-injection). Results were given in *Fig. 6* and *Fig. 7*.

Biodistribution Studies in Female Albino Wistar Rats

The experiments were performed on female Albino Wistar rats infected. The biodistribution data are expressed as percentage of injected radioactivity per gram of tissue (%ID/g) for selected organs as the mean value of three rats. The ^{99m}Tc-TMH injected into the tail vein of the animal in the activity amount of 37 MBq of ^{99m}Tc-TMH per rat. In the first stage of the biodistribution process, rat was sacrificed at 30, 120, and 240 min post injection under dense ethyl ether anesthesia, the abdominal region of the rat was incised, and the organs were taken. All tissues were weighed and counted for radioactivity with a Cd/Te detector. Results of biodistribution study were summarized in *Table 1*.

Histopathology Studies

Tissue samples were fixed in 10% formalin solution for 24-48 h. Then, routine paraffin embedding procedures were used

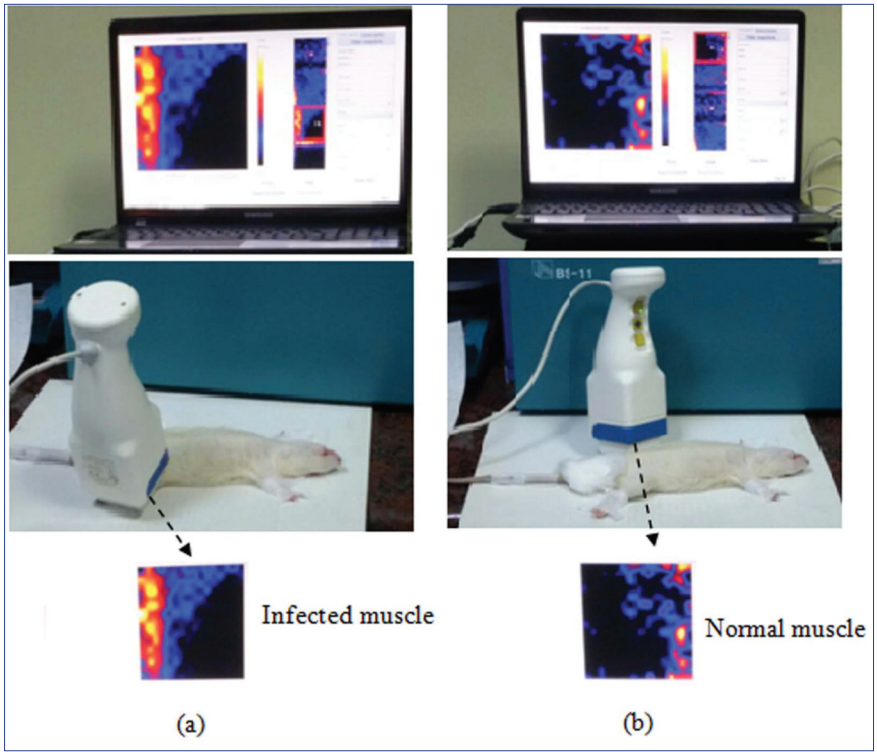

Fig 7. Portable gamma camera imaging study of ^{99m}Tc-TMH, which was administered to a rat via the tail vein in 30 min (The mixture of xylazine and ketamine anesthesia was used in the imaging studies. Static image was obtained from posterior projection following the administration of the ^{99m}Tc-TMH)

and 5 µm thick sections were cut from embedded tissues.

Paraffin Embedding Procedure

Fixed tissues washed with tap water for one night in order to remove the fixative solution. Then they were dehydrated through a graded ethanol series (60%, 70%, 80% and 95%), cleared in xylene and embedded in paraffin. Sections with 5 µm thickness were cut by rotary microtome (RM 2135, Leica) and were stained with hematoxylin-eosin for histochemical analyses.

Hematoxylin-Eosin Staining Procedure

Sections dewaxed under 60ºC overnight were immersed in xylene for 1 h and then rehydrated through a graded series of ethanol (95%, 80%, 70%, and 60%) for 2 min in each concentration and they were then washed in tap water for 5 min. Sections were stained with hematoxylin (01562E, Surgipath, Bretton, Peter Borough, Cambridge Shire) and washed in tap water for 5 min. Then sections were stained with eosin (01602E, Surgipath, Bretton, Peter Borough, Cambridge Shire) and washed in tap water for 5 min. After sections dehydrated with 80% and 95% alcohol and immersed in xylene and mounted with entellan (UN 1866, Merck, Darmstadt, Germany).

Statistical Analysis

The calculation of means and standard deviations were made on Microsoft Excel. One-way analysis of variance was used to determine statistical significance. Differences at the 95% confidence level ($P<0.05$) were considered significant.

RESULTS

Radiochemical purity and stability of ^{99m}Tc-TMH complex were assessed by thin layer and HPLRC methods. In thin layer chromatography using Acetone-water (9:1) as the solvent, free pertechnetate moved with the solvent front (R_f = 0.9), while ^{99m}Tc-TMH and reduced hydrolyzed technetium remained at the origin as seen in *Fig. 2*. Reduced hydrolyzed technetium was determined by using ethanol: water: ammonium hydroxide mixture (2:5:1) or 5 N NaOH as the mobile phase, where reduced hydrolyzed technetium remains at the origin (R_f = 0) while other species migrate with the solvent front (R_f=1). The radiochemical yield was determined as 96±2%. Also, radiochemical purity of ^{99m}Tc-THH was confirmed by HPLRC as seen in *Fig. 3*. Retention times of radio components, TcO_4^- and ^{99m}Tc-TMH, were found to be 4.105±0.158 and 9.202±0.102 (min), respectively.

Effect of pH

As shown in *Fig. 4*, at pH 1 the labeling yield of ^{99m}Tc-TMH complex was equal to 0 and this yield increased with increasing the pH of the reaction mixture where pH 10 gave the maximum labeling yield of 96%. By increasing the pH greater than 10, the labeling yield remained constant.

Stability Test

As seen in *Fig. 5*, incubation of the preparation containing ^{99m}Tc-TMH in normal serum for 180 min at 37ºC resulted in a small decrease in the yield of ^{99m}Tc-TMH (85±2%) determined by TLRC.

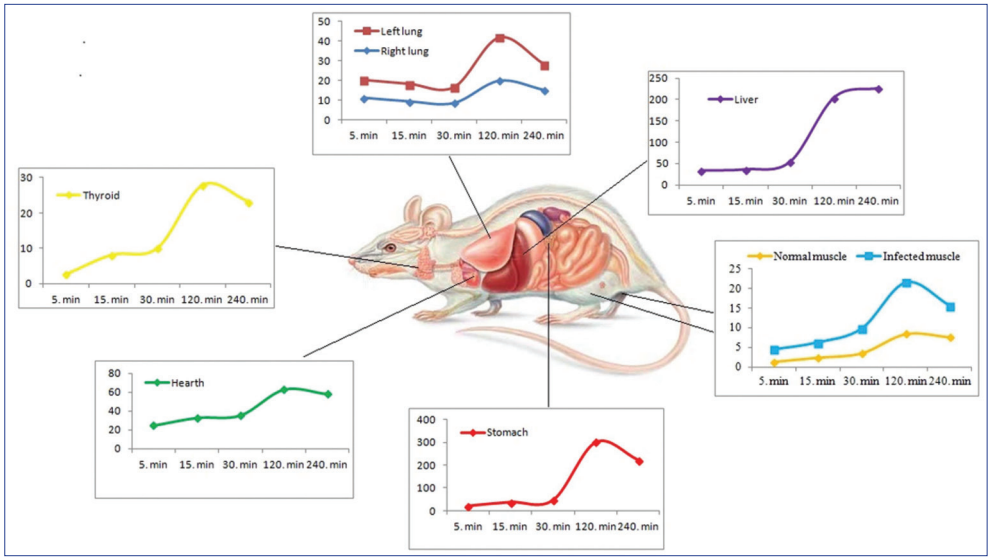

Fig 8. Region of interest (ROI) values of ^{99m}Tc-TMH at different time intervals

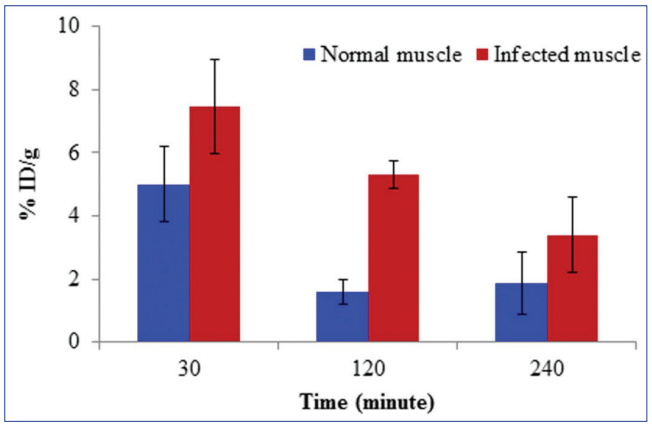

Fig 9. % ID/g values of ^{99m}Tc-TMH normal muscle and ınfected muscle in 30, 120 and 240 minute (n = 3); error bars mean standard deviation; %ID = percent of the injected dose per gram tissue

in 30 min as seen in *Fig. 6* and *Fig. 7*.

We also observed that ^{99m}Tc activity in the chest region and the abdominal region increased correspondingly with time. It may be interpreted that radiation signal in the chest region is possibly due to the activity in the lungs with reference to ROI values displayed in *Fig. 8*. In addition to this, the clear ^{99m}Tc uptake in the abdominal region is most probably the sign of high activity in the stomach, the liver and the intestines. ROI values indicate that the highest ^{99m}Tc activity is observed in the stomach in all time intervals, thus the activity in the abdominal region is most likely due to the stomach. The reason of such high ^{99m}Tc activity in the stomach can be explained in a way that the ^{99m}Tc eliminated from ^{99m}Tc-TMH showed high accumulation in this organ [29,30].

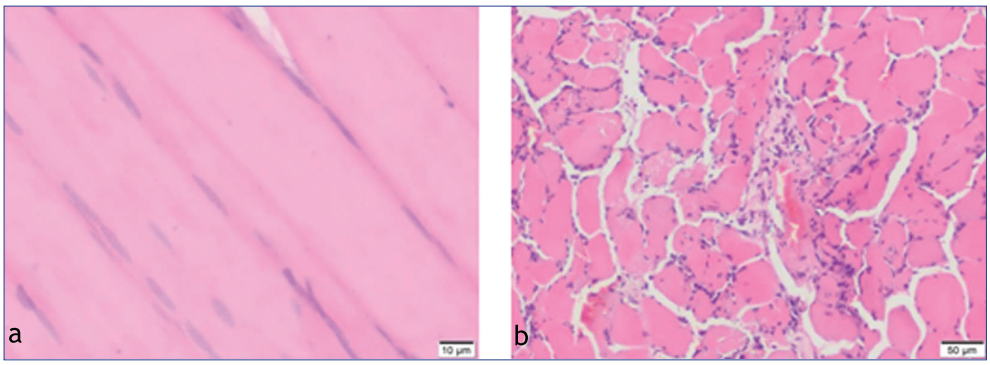

Fig 10. (a) Healthy rat muscle and (b) infected rat muscle microscopic appearance viewed by microscopy

Imaging Studies

After the administration of ^{99m}Tc-TMH to rats, static images were obtained by using a dual head gamma camera (Infinia General Electric) and handheld USB-Gamma Camera (CrystalCam). Static image of ^{99m}Tc-TMH in male rats demonstrated that important radiation signals are present in the infected site at first glance

Biodistribution Studies

The biodistribution data of the ^{99m}Tc-TMH radio-complex in various organs of the rats were given in *Table 1*. After 30 min the uptake of the ^{99m}Tc-TMH as ID/g% in the infected muscle (INM) and normal muscle (NM) of the rats were 7.5±1.5% and 5.00±1.2%, respectively. An decrease in the uptake of the activity in the INM up

to 5.3±0.5% was observed after 120 min, however, the uptake went down to 3.4±1.9% within 240 min. In the NM a significant decrease in the activity of ^{99m}Tc-TMH radio-complex was observed. In the INM/NM ratio a desirable behavior was observed as the values for the INM/NM increased up to 10.6 as seen in *Fig. 9*. Activity of the ^{99m}Tc-TMH radio-complex in blood significantly increased from 7.89±1.45% to 26.2±12.5% within 120 min. The activity in the liver was initially high but within 120 min it decreased to 7.5±4.0% from 165.7±27.5%. Similar distribution was observed in the lung and the stomach. In the stomach the activity initially was quite low but within 120 min it reached 208.3±11.8%. The disappearance of the ^{99m}Tc-TMH radio-complex from blood and liver and appearance in the kidney confirmed the normal route of excretion of the ^{99m}Tc-TMH complex. 10.6 fold higher accumulation of ^{99m}Tc-TMH complex in the *Staphylococcus aureus* (SA) infected muscle of the model rat [31-33].

Histopathology Results

As for histopathology studies, striation of muscle was normal and there was no polymorphonuclear leukocyte (PMNL) infiltration and the connective tissue was also normal between the fibers in the TMP 30 normal muscle group. Striation of muscle was normal but there was disintegration of muscle fibers in the TMP 120 normal muscle group. In the TMP 120 infected muscle group, the architecture of the muscle fiber was normal but the striation was not seen in some of the muscle fibers. Microscopic images of healthy and infected rat muscle were given in *Fig. 10*.

DISCUSSION

^{99m}Tc may be formed by interactions between electron donor atoms such as nitrogen, oxygen, sulfur and reduced technetium. Due to presence of electron donor atoms in TMH structure the reduced sodium pertechnetate can easily react with this ligand and a complex is formed. So, we found high radiolabeling yield for ^{99m}Tc-TMH as about 96%.

The effect of pH on radiochemical purity was examined at pH 1.0-13.0. According to the experiments results the pH of the reaction medium was found to play an important role in the labeling process. While keeping other reaction conditions constant and varied the pH of the reaction from 1.0 to 13.0 radiochemical purity was highly increased.

The results presented herein demonstrate that ^{99m}Tc-TMH scintigraphy can preferentially localize infection in rats, even in the absence of clinical signs of infectious processes. As demonstrated by *in vivo* scintigraphy, the presence of bacteria in the ROIs was significantly associated with high levels of radioactivity at both evaluation times, namely, 120 and 240 min after injection.

According to Wagner grading system (referans) SA infected rats were Grade 2. The infection was limited to the skin, fascia and muscle. There was no abscess or bone infection.

The use of radiolabeled antibiotics represents a novel approach in the differentiation of infection from aseptic inflammation. Since the antibiotics are bound to or metabolized by bacteria, the amount of radioactivity measured in the ROI is proportional to the number of microorganisms present at the site. Fluoroquinolone antibiotics, which include ciprofloxacin, sparfloxacin and levofloxacin, are the most commonly used scintigraphic markers of infection. However, the results obtained with these antibiotics are contradictory and exhibit low reproducibility. Thus, Shah et al.[26] reported that scintigraphic imaging with ^{99m}Tc-ciprofloxacin cannot distinguish aseptic processes from osteomyelitis and suggested that this limitation is due to the pharmacodynamic properties of the antibiotic including low molecular weight (331.3), low degree of interaction with plasma proteins (20-40%) and protracted biological half-life (4.5 h).

Imaging of infections is an important application, as well as their therapy, but conventional radiological methods such as X-ray, ultrasound, computed tomography (CT) and magnetic resonance imaging (MRI) are not specific to distinguish inflamed and infected areas. For this reason, there is a need to develop alternative strategies. Imaging of inflammations with radiopharmaceuticals is the most challenging technique due to its specificity at infection sites [28,33]. When preparing the radiopharmaceuticals, various radionuclides (Ga-67, Tc-99m, In-111, F-18, etc.) are used to label small molecules (radiolabeled antimicrobial peptides, antibiotics, antibiotic peptides and chemotactic peptides). New radiolabeled compounds have been developed for infection imaging in the last year. In this study, because TMH has an antimicrobial effect and its structure is suitable to label using ^{99m}Tc, we evaluated the probability that ^{99m}Tc-TMH could be useful as a radiopharmaceutical for infection imaging.

^{99m}Tc-TMH a new radioantibiotic complex prepared by using 100 µg TMH, 5 µg of $SnCl_2.2H_2O$, 37 MBq (1 mCi) of $Na^{99m}TcO_4$, at pH 10 showed promising *in-vitro* radiochemical purity yield, soaring permanence, fitting *in-vivo* biodistribution infected rats and scintigraphic precision in SA infected rats. In our opinion the ^{99m}Tc-TMH complex meet the requirements of an infection imaging agent; therefore, we recommend the ^{99m}Tc-TMH complex prepared aseptically for *in-vivo* assessment of SA infection.

Acknowledgments

The authors are thankful for the financial support from

the Manisa Celal Bayar University Research Fund (Contract No. 2015-101).

REFERENCES

1. Elbashir S, Parveen S, Schwarz J, Rippen T, Jahncke M, DePaola A: Seafood pathogens and information on antimicrobial resistance: A review. *Food Microbiol,* 70, 8593, 2018. DOI: 10.1016/j.fm.2017.09.011

2. Levy SB, Marshall B: Antibacterial resistance worldwide: Causes, challenges and responses. *Nat Med*, 10, S122-S129, 2004. DOI: 10.1038/nm1145

3. Sefton AM: Mechanisms of antimicrobial resistance-their clinical relevance in the new millennium. *Drugs,* 62, 557-566, 2002.

4. Kaur A, Khan IA, Banipal PK, Banipal TS: Deciphering the complexation process of a fluoroquinole antibiotic, levofloxacin, with bovine serum albumin in the presence of additives. *Spectrochim Acta A Mol Biomol Spectrosc*, 191, 259-270, 2018. DOI: 10.1016/j.saa.2017.10.017

5. Correa A, del Campo R, Escandon-Vargas K, Perenguez M, Rodriguez-Banos M, Hernandez-Gomez C, Pallares C, Perez F, Arias CA, Canton R, Villegas MV: Distinct genetic diversity of carbapenem-resistant *Acinetobacter baumannii* from Colombian Hospitals. *Microb Drug Resist*, 24 (1): 48-54, 2018. DOI: 10.1089/mdr.2016.0190

6. Ferk, F, Misik M, Grummt T, Majer B, Fuerhacker M, Buchmann C, Vital M, Uhl M, Lenz K, Grillitsch B, Parzefall W, Nersesyan A, Knasmuller S: Genotoxic effects of wastewater from an oncological ward. *Mutat Res-Gen Tox En,* 672 (2): 69-75, 2009. DOI: 10.1016/j.mrgentox.2008.08.022

7. Baquero F, Martínez JL, Cantón R: Antibiotics and antibiotic resistance inwater environments. *Curr Opin Biotechnol*, 19, 260-265, 2008. DOI: 10.1016/ j.copbio.2008.05.006

8. Nieto A, Borrull F, Marce RM, Pocurull E: Selective extraction of sulfonamides, macrolides and other pharmaceuticals from sewage sludge bypressurized liquid extraction. *J Chromatogr A*, 1174, 125-131, 2007. DOI: 10.1016/j.chroma.2007.09.068

9. De Paula FC, De Pietro AC, Cass QB: Simultaneous quantification of sulfamethoxazole and trimethoprim in whole egg samples by column-switching high-performance liquid chromatography using restricted access media column for on-line sample clean-up. *J Chromatogr A,* 1189, 221-226, 2008. DOI: 10.1016/j.chroma.2007.08.046

10. Gobel A, McArdell CS, Suter MJF, Giger W: Trace determination of macrolide and sulfonamide antimicrobials, a human sulfonamide metabolite, and trimethoprim in waste water using liquid chromatography coupled toelectrospray tandem mass spectrometry. *Anal Chem*, 76, 4756-4764, 2004. DOI: 10.1021/ac0496603

11. Gobel A, Thomsen A, McArdell CS, Joss A, Giger W: Occurrence andsorption behavior of sulfonamides, macrolides, and trimethoprim in activated sludge treatment. *Environ Sci Technol*, 39, 3981-3989, 2005. DOI: 10.1021/es048550a

12. Chang H, Hu J, Asami M, Kunikane S: Simultaneous analysis of 16sulfonamide and trimethoprim antibiotics in environmental waters by liquid chromatography-electrospray tandem mass spectrometry. *J Chromatogr A*, 1190, 390-393, 2008. DOI: 10.1016/j.chroma.2008.03.057

13. Phuong Hoa PT, Nonaka L, Hung VP, Suziki S: Detection of the *sul1*, *sul2,* and *sul3* genes in sulfonamide-resistant bacteria from waste water and shrimp ponds of north Vietnam. *Sci Total Environ*, 405, 377-384, 2008. DOI: 10.1016/j.scitotenv.2008.06.023

14. Xu J, Xu Y, Wang H, Gua C, Qiu H, He Y, Zhang Y, Li X, Meng W: Occurrence of antibiotics and antibiotic resistance genes in a sewage treatment plant and its effluent-receiving river. *Chemosphere,* 119, 1379-1385, 2015. DOI: 10.1016/j.chemosphere.2014.02.040

15. Szczepanowski R, Linke B, Krahn I, Gartemann KH, Gützkow T, Eicher W, Pühler A, Schlüter A: Detection of 140 clinically relevant antibiotic-resistance genes in the plasmid metagenome of waste water treatment plant bacteria showing reduced susceptibility to selected antibiotics. *Microbiology,* 155, 2306-2319, 2009. DOI: 10.1099/mic.0.028233-0

16. Gallagher H, Ramsay SC, Barnes J, Maggs J, Cassidy N, Katheesan: Neutrophil labeling with [^{99m}Tc]-technetium stannous colloid is complement receptor 3-mediated and increases the neutrophil priming response to lipopolysaccharide. *Nucl Med Biol*, 33, 433-437, 2006. DOI: 10.1016/j.nucmedbio.2005.12.014

17. Stumpe KDM, Dazzi H, Schaffner A, Von Schulthess GK: Infection imaging using whole-body FDG-PET. *Eur J Nucl Med*, 27, 822-826, 2000. DOI: 10.1007/s002590000277

18. Burke SL, Rose WE: New pharmacological treatments for methicillin-resistant *Staphylococcus aureus* infections. *Expert Opin Pharmacother*, 15 (4): 483-491, 2014. DOI: 10.1517/14656566.2014.876991

19. Shah SQ, Khan AU, Khan MR: Radiosynthesis and biodistribution of ^{99m}Tc-rifampicin: A novel radiotracer for *in-vivo* infection imaging. *Appl Radiat Isot*, 68, 2255-2261, 2010. DOI: 10.1016/j.apradiso.2010.05.014

20. Shah SQ, Khan AU, Khan MR: ^{99m}Tc-novobiocin: A novel radiotracer for infection imaging. *Radiochimica Acta,* 99, 53-58, 2011. DOI: 10.1524/ract.2011.1790

21. Shah SQ, Khan AU, Khan MR: Radiosynthesis, biodistribution and scintigraphy of the ^{99m}Tc-teicoplanin complex in artificially infected animal models. *J Label Compd Radiopharm*, 54, 145-152, 2010. DOI: 10.1002/jlcr.1834

22. Shah SQ, Khan MR: ^{99m}Tc$(CO)_3$-tosufloxacin dithiocarbamate complexation and radiobiological evaluation in male Wister rat model. *J Radioanal Nucl Chem*, 288, 485-490, 2011. DOI: 10.1007/s10967-010-0943-4

23. Shah SQ, Khan MR: Synthesis of the ^{99m}Tc$(CO)_3$- trovafloxacin dithiocarbamate complex and biological evaluation in artificially methicillin-resistant *Staphylococcus aureus* infected rats model. *J Radioanal Nucl Chem*, 288, 297-302, 2011. DOI: 10.1007/s10967-010-0914-9

24. Shah SQ, Khan MR: (99m)Tc-prulifloxacin in artificially infected animals: Radiosynthesis and biological evaluation of 99mTc-prulifloxacin in artificially infected animals. *Nuklearmedizin,* 50, 134-140, 2011. DOI: 10.3413/Nukmed-0334-10-07

25. Shah SQ, Khan MR: Radiosynthesis and characterization of the 99mTc-fleroxacin (99mTc-FXN) complex: A novel *Escherichia coli* infection imaging agent. *Transit Met Chem,* 36, 283-288, 2011.

26. Shah SQ, Khan MR: Synthesis of techentium-99 m labeled clinafloxacin (^{99m}Tc-CNN) complex and biological evaluation as a potential *Staphylococcus aureus* infection imaging agent. *J Radioanal Nucl Chem*, 288, 423-428, 2011.

27. Özdemir Dİ, Asikoglu M, Ozkilic H, Yılmaz F, Limoncu MH, Ayhan S: ^{99m}Tc-doxycycline hyclate: A new radiolabeled antibiotic for bacterial infection imaging. *J Label Compd Radiopharm*, 2013 DOI: 10.1002/jlcr.3135

28. Uyaroğlu Ö, Demiroğlu H, Topal G, Parlak Y, Gümüşer FG, Türköz EU, Tekin V, Ateş B, Ünak P, Avcıbaşı U: Radiosynthesis and biodistribution of ^{99m}Tc- Sulfamethoxazole: A novel molecule for in-vivo infection imaging. *Med Chem*, 26, 3149-3157, 2017. DOI: 10.1007/s00044-017-2009-4

29. Li CH, Chen Y, Zhang CH, Dong Z, Wang Z, Zhao SN, Wang YX, LV ZY, Zhang PL: Observation of clinical efficacy of rt-PA intravenous thrombolytic treatment for patients combined with grade 0-1 diabetic foot by Wagner classification and acute ischemic stroke. *Eur Rev Med Pharmacol Sci*, 20, 5168-5173, 2016.

30. Palestro CJ, Love C, Tronco GG, Tomas MB: Role of radionuclide imaging in the diagnosis of postoperative infection. *Radiographics*, 20, 1649-1660, 2000. DOI: 10.1148/radiographics.20.6.g00nv101649

31. Diniz SO, Rezende CM, Serakides R, Ferreira RL, Ribeiro TG, Martin-Comin J, Cardoso VN: Scintigraphic imaging using technetium-99m-labeled ceftizoxime in an experimental model of acute osteomyelitis in rats. *Nucl Med Commun*, 29, 830-836, 2008. DOI: 10.1097/MNM.0b013e3283000514

32. Liberatore M, Fiore V, D'Agostini A, Prosperi D, Iurilli AP, Santini C, Baiocchi P, Galiè M, Di Nucci GD, Sinatra R: Sternal wound infection revisited. *Eur J Nucl Med*, 27, 660-667, 2000. DOI: 10.1007%2Fs002590050560

33. Ertay T, Ünak P, Eren MŞ, Müftüler FZB, Özdoğan Ö, Ülker Ö, Yeşilağaç R, Durak H: A New ^{99m}Tc labeled peptide: ^{99m}Tc β-casomorphin 6, biodistribution and imaging studies on rats. *Kafkas Univ Vet Fak Derg,* 23 (1): 15-22, 2017. DOI: 10.9775/kvfd.2016.15691